Interactions of Isopenicillin N Synthase with Cyclopropyl-Containing Substrate Analogues Reveal New Mechanistic Insight[†,‡]

Annaleise R. Howard-Jones,[§,||] Jonathan M. Elkins,[§,⊥] Ian J. Clifton, Peter L. Roach,[#] Robert M. Adlington, Jack E. Baldwin,* and Peter J. Rutledge*[,▽]

Chemistry Research Laboratory, University of Oxford, Mansfield Road, Oxford OX1 3TA, U.K.

Received November 8, 2006; Revised Manuscript Received February 6, 2007

ABSTRACT: Isopenicillin N synthase (IPNS), a non-heme iron oxidase central to penicillin and cephalosporin biosynthesis, catalyzes an energetically demanding chemical transformation to produce isopenicillin N from the tripeptide δ-(L-α-aminoadipoyl)-L-cysteinyl-D-valine (ACV). We describe the synthesis of two cyclopropyl-containing tripeptide analogues, δ-(L-α-aminoadipoyl)-L-cysteinyl-β-methyl-D-cyclopropylglycine and δ-(L-α-aminoadipoyl)-L-cysteinyl-D-cyclopropylglycine, designed as probes for the mechanism of IPNS. We have solved the X-ray crystal structures of these substrates in complex with IPNS and propose a revised mechanism for the IPNS-mediated turnover of these compounds. Relative to the previously determined IPNS−Fe(II)−ACV structure, key differences exist in substrate orientation and water occupancy, which allow for an explanation of the differences in reactivity of these substrates.

Formation of the penicillin core of isopenicillin N (IPN[1]) **2** from the tripeptide δ-(L-α-aminoadipoyl)-L-cysteinyl-D-valine (ACV) **1** is catalyzed by the enzyme isopenicillin N synthase (IPNS) (Scheme 1A) (*1*). This is a four-electron oxidative bicyclization, resulting in formation of both the β-lactam and thiazolidine rings of the IPN product. The complete reduction of dioxygen to water drives formation of the strained bicyclic ring system. It has been shown that the enzyme utilizes one molecule of dioxygen for every molecule of IPN produced (*2*). The mechanism of action of IPNS is believed to proceed *via* initial closure of the β-lactam ring (*3*), with concomitant formation of an iron(IV)−oxo intermediate (Scheme 2A) (*4*). This high-valent iron species is then thought to mediate closure of the thiazolidine ring through abstraction of the D-valinyl β-hydrogen.

Scheme 1: Turnover of (A) ACV **1**; (B) AC-Me-cpG **3**; and (C) ACcpG **5** by IPNS, as Observed in Solution-Phase Experiments[a]

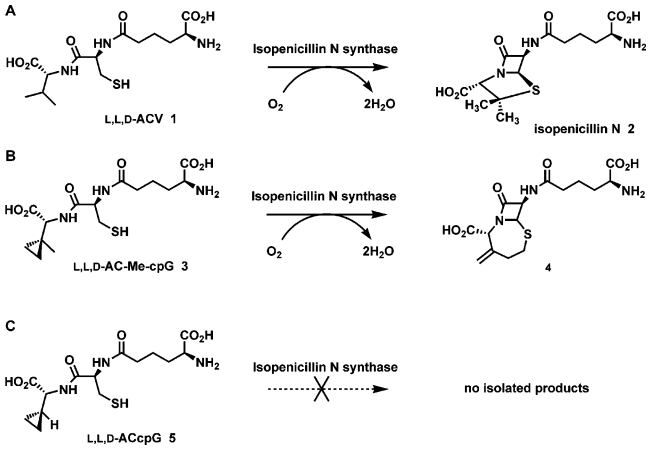

[a] Reference *18,* Domayne-Hayman, B. P., and Baldwin, J. E., unpublished.

Aspergillus nidulans IPNS was first crystallized in 1995 (*5*), which allowed the determination of a structure for the IPNS−Mn(II) complex (*6*). Later work led to structures of the IPNS−Fe(II)−ACV, IPNS−Fe(II)−ACV−NO (*7*), and IPNS−Fe(II)−IPN complexes (*4*) being solved. These structures contributed greatly to our understanding of the architecture of the active site and enzyme−substrate interactions that dictate the reaction pathway. Since that time, further advances in mechanistic understanding have been made through cocrystallization of IPNS with modified substrate analogues to study reaction cycle intermediates and shunt metabolites (*4*, *8*−*14*). Prior to the crystallization of IPNS, mechanistic information on the enzyme was derived from extensive spectroscopic investigations (*15*, *16*) and incubation

[†] This work was supported in part by the Medical Research Council (MRC), the Biotechnology and Biological Sciences Research Council (BBSRC), the Engineering and Physical Sciences Research Council (EPSRC) UK, and the Wellcome Trust. A.R.H.-J. was supported by a Rhodes Scholarship from the Rhodes Trust, Oxford, U.K.

[‡] Crystallographic coordinates and structure factors have been deposited in the Protein Data Bank (PDB) under Accession Nos. 2IVI and 2IVJ.

* To whom correspondence should be addressed. Dr. Peter Rutledge: tel, +61 2 93515020; fax, +61 2 93513329; e-mail, p.rutledge@chem.usyd.edu.au. Professor Sir Jack Baldwin: tel, +44 1865 275670; fax, +44 1865 285002; e-mail, jack.baldwin@chem.ox.ac.uk.

[§] These authors contributed equally to this work.

[||] Present address: Harvard Medical School, Department of Biological Chemistry & Molecular Pharmacology, 240 Longwood Avenue, Boston, MA 02115.

[⊥] Present address: Structural Genomics Consortium, University of Oxford, Botnar Research Centre, Oxford OX3 7LD, U.K.

[#] Present address: School of Chemistry, University of Southampton, Highfield, Southampton SO17 1BJ, U.K.

[▽] Present address: School of Chemistry F11, University of Sydney, NSW 2006, Australia.

[1] Abbreviations: AC dipeptide, (*N*-*tert*-butyloxycarbonyl-α-*p*-methoxybenzyl-δ-(L-α-aminoadipoyl)-*S*-benzhydryl-L-cysteine; AC-Me-cpG, δ-(L-α-aminoadipoyl)-L-cysteinyl-β-methyl-D-cyclopropylglycine; AC-cpG, δ-(L-α-aminoadipoyl)-L-cysteinyl-D-cyclopropylglycine; ACV, δ-(L-α-aminoadipoyl)-L-cysteinyl-D-valine; IPN, isopenicillin N; IPNS, isopenicillin N synthase.

10.1021/bi062314q CCC: $37.00
Published on Web 03/31/2007

Scheme 2: (A) Mechanism for Turnover of ACV **1** by IPNS (*7*) and (B) Proposed Mechanism for Turnover of AC-Me-cpG **3** by IPNS

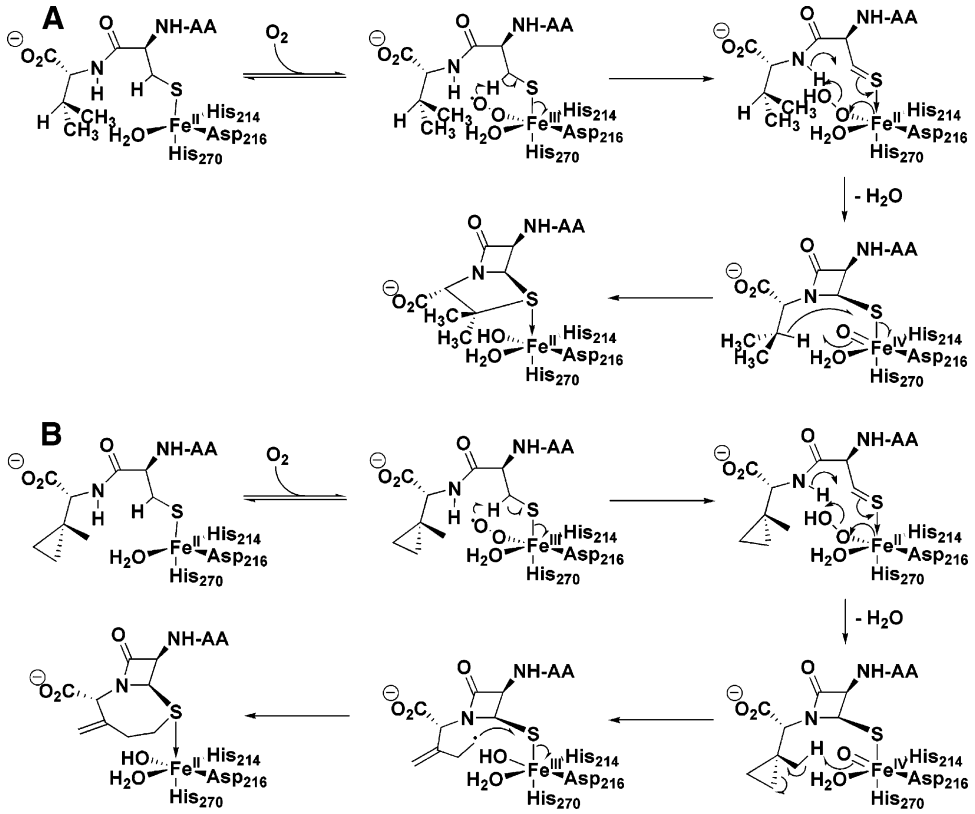

experiments of IPNS with a diverse range of substrate analogues (*17*).

The cyclopropyl group was incorporated into tripeptide substrate analogues to probe various aspects of IPNS catalysis (*18*, Domayne-Hayman, B. P., and Baldwin, J. E., unpublished). Turnover of the tripeptide δ-(L-α-aminoadipoyl)-L-cysteinyl-β-methyl-D-cyclopropylglycine (AC-Me-cpG) **3** (Scheme 1B) by IPNS was studied to probe the putative radical nature of the turnover cycle (*18*). If a radical intermediate is involved in thiazolidine ring closure, the cyclopropyl ring should open to give an unsaturated macrocyclic product. Indeed, these studies showed that incubation of AC-Me-cpG **3** with IPNS in solution yielded an unsaturated (*4*, *7*) fused bicyclic product **4** (Scheme 1B) (*18*). At that time, however, without the benefit of crystallographic information, many aspects of the mechanism of this IPNS-mediated reaction were unclear. Several mechanistic alternatives were put forward, including an "ene"-type reaction to facilitate opening of the three-membered ring and a mechanism involving direct insertion of iron into a C−H bond (Scheme 3) (*19*, *20*).

The interaction of δ-(L-α-aminoadipoyl)-L-cysteinyl-D-cyclopropylglycine (ACcpG) **5** (Scheme 1C) with IPNS was also studied with the aim of probing the IPNS turnover cycle (Domayne-Hayman, B. P., and Baldwin, J. E., unpublished). This substrate was designed to inhibit "valinyl" β-hydrogen abstraction, which is believed to occur during thiazolidine formation. In these incubation experiments, no β-lactam products were isolated (Scheme 1C), indicating that ACcpG was most likely not turned over by IPNS.

Herein we examine the interaction of IPNS with the two cyclopropyl-containing tripeptides AC-Me-cpG **3** and AC-cpG **5** using X-ray crystallography. The two substrates have been prepared by two distinct pathways allowing exploration of different synthetic strategies to cyclopropyl-bearing tripeptides. We look at the binding of these substrate analogues within the active site by solving crystal structures of the anaerobic IPNS−Fe(II)−substrate complexes, which reveal key differences in orientation between these two substrates and that of ACV in the IPNS−Fe(II)−ACV complex (*7*). These structures, in combination with other recent mechanistic studies on IPNS (*8*) and related enzymes (*15*, *22*), allow revision of the mechanism for the turnover of cyclopropyl-containing substrates by IPNS.

MATERIALS AND METHODS

Synthesis of Tripeptides. 1. Synthesis of δ-(L-α-Aminoadipoyl)-L-cysteinyl-β-methyl-D-cyclopropylglycine 3. DL-β-Methylcyclopropylglycine **6** was assembled by TPAP/NMO-mediated oxidation of 1-methylcyclopropanemethanol to give the corresponding aldehyde, followed by introduction of the amine functionality using 4,4′-dimethoxybenzhydrylamine, and then the carboxylate using trimethylsilyl cyanide with 6 M hydrochloric acid hydrolysis (*23*). After BOC-protection of the amino group, the carboxylate was protected as its benzhydryl ester using diphenyldiazomethane, after which the BOC group was removed to give compound **7** for coupling to the partially protected AC dipeptide (*N*-*tert*-butyloxycarbonyl-α-*p*-methoxybenzyl-δ-(L-α-aminoadipoyl)-*S*-benzhydryl-L-cysteine (*8*, *24*)). An EEDQ-mediated condensation was used to couple compound **7** to the AC dipeptide, giving compound **10**. Global deprotection of **10** using TFA and anisole (*33*) and reversed-phase HPLC purification [0 → 25% acetonitrile in 10 mM $NH_4 \cdot HCO_3$,

Scheme 3: Previously Proposed Mechanisms for Turnover of AC-Me-cpG **3** by IPNS[a]

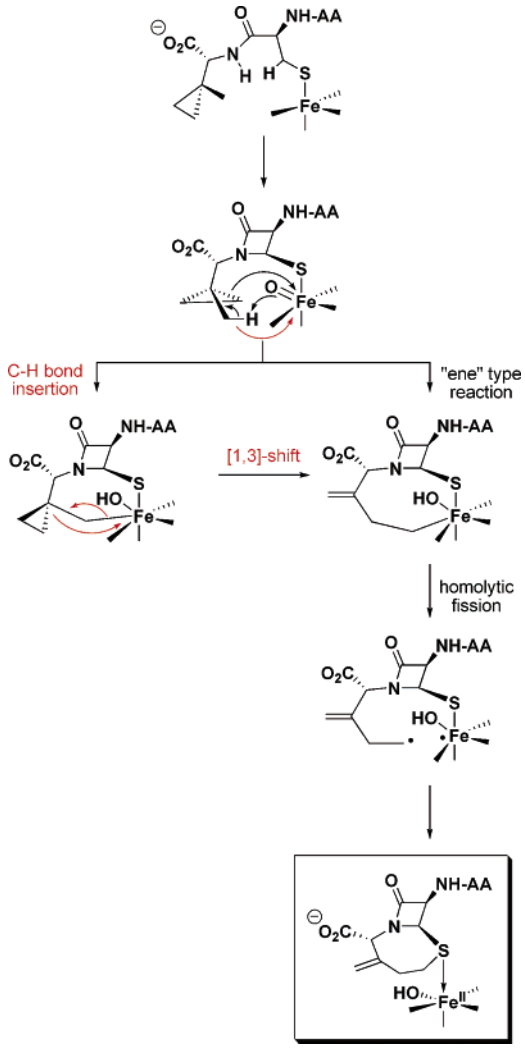

[a] References *19*, *20*. Red arrows indicate proposed mechanism for C−H bond insertion route; black arrows denote "ene"-type reaction pathway.

Hypersil 5 μ C18 column, 250 × 10 mm internal diameter; λ = 254 nm; 4 mL/min] gave the tripeptide **3** for crystallographic analysis: ^{1}H (500 MHz, D_2O) δ 4.50−4.47 (1H, m, 1 × H_α), 3.66−3.62 (2H, m, 2 × H_α), 2.86−2.77 (2H, m, 2 × H_β(Cys)), 2.34−2.31 (2H, m, 2 × H_δ(α-AA)), 1.82−1.76 and 1.67−1.58 (2 × 2H, 2 × m, 2 × H_β and 2 × H_γ-(α-AA)), 0.93 (3H, s, $(CH_3)_\gamma$(Me-cpG)), 0.65−0.62, 0.45−0.41, 0.39−0.35 and 0.30−0.27 (4 × H, 4 × m, 4 × H_γ(Me-cpG)); *m/z* (ES$^+$) 376.5 (MH^+, 100%).

*2. Synthesis of δ-(*L*-α-Aminoadipoyl)-*L*-cysteinyl-*D*-cyclopropylglycine **5**.* Following protection of both the amine and carboxylate functionalities of D-glutamic acid (using the BOC and *p*-methoxybenzyl protecting groups respectively), the D-vinylglycine moiety **8** was prepared by copper(II)/lead-(IV)-mediated oxidative decarboxylation of the δ-carboxylate (*34*−*36*). Palladium-catalyzed carbene insertion using diazomethane (*37*, *38*) afforded the cyclopropyl moiety, and subsequent removal of the BOC group with *p*-toluenesulfonic acid gave the partially protected cyclopropylglycine **9**. Compound **9** was coupled to the preassembled, partially protected AC dipeptide using an EDCI/HOBT protocol (*27*, *39*), giving compound **11** [*m/z* 890 $(M + Na)^+$, 100%; 868 MH^+, 10%]. Global deprotection of **11** using TFA and anisole (*33*) followed by purification by reversed-phase HPLC [10 mM $NH_4{\cdot}HCO_3$, Hypersil 5 μ C18 column, 250 × 10 mm internal diameter; λ = 254 nm; 4 mL/min] afforded the pure tripeptide **5**: t_R 4 min 50 s; ^{1}H NMR (400 MHz, D_2O) δ 4.39 (1H, t, *J* 6.5 Hz, H_α(Cys)), 3.60 (1H, t, *J* 6.0 Hz, H_α(α-AA)), 3.43 (1H, d, *J* 9.0 Hz, H_α(cpG)), 2.80−2.71 (2H, m, 2 × H_β(Cys)), 2.27 (2H, t, *J* 7.0 Hz, 2 × H_δ-(α-AA)), 1.75−1.69 (2H, m, 2 × H_β(α-AA)), 1.62−1.49 (2H, m, 2 × H_γ(α-AA)), 1.02−0.93 (1H, m, H_β(cpG)), 0.50−0.43 (1H, m, 1 × H_γ(cpG)), 0.43−0.37 (1H, m, 1 × H_γ-(cpG)), 0.34−0.28 (1H, m, 1 × H_γ(cpG)), 0.16−0.10 (1H, m, 1 × H_γ(cpG)); ^{13}C NMR (101 MHz, D_2O) δ 178.2, 176.3 (2 × CO_2H), 174.8, 171.4 (2 × NHCO), 59.5 (C_α(cpG)), 55.9 (C_α(Cys)), 54.7 (C_α(α-AA)), 35.0 (C_δ(α-AA)), 30.1 (C_β-(α-AA)), 25.8 (C_β(Cys)), 21.1 (C_γ(α-AA)), 13.1 (C_β(cpG)), 3.4, 2.7 (2 × C_γ(cpG)).

Crystallization Experiments. Crystals of ACcpG **5** or AC-Me-cpG **3**, IPNS, and Fe(II) were grown using the hanging drop method under anaerobic conditions at 17 °C in a Belle Technology glovebox (<0.4 ppm O_2) (*28*). Crystals were prepared for data collection by exchanging into a cryoprotectant buffer (a 1:1 mixture of well buffer with a saturated solution of Li_2SO_4 in 40% glycerol) and flash-freezing in liquid nitrogen.

Data Collection. Data were collected using synchrotron X-ray radiation (0.933 or 0.935 Å) and an ADSC Quantum 4 CCD detector at beamlines ID14-EH2 or ID14-EH3 of the European Synchrotron Research Facility (ESRF), Grenoble, France. Crystals were maintained at 100 K using an Oxford Cryostream.

Structure Determination. Data were processed using MOSFLM (*40*) and the CCP4 suite of programs (*41*). An initial model was obtained by rigid body refinement of the protein atoms of the previously determined IPNS−Fe(II)−L,L,D-ACV structure (*7*) against the new data. Model refinement was carried out using REFMAC (*41*), and electron density maps were interpreted using the program O (*42*). Substrate atoms were added at advanced stages of refinement. Crystallographic coordinates and structure factors have been deposited in the Protein Data Bank (PDB) under Accession Nos. 2IVI (IPNS−Fe(II)−(AC-Me-cpG) complex) and 2IVJ (IPNS−Fe(II)−ACcpG complex).

RESULTS

*Synthesis of AC-Me-cpG **3** and ACcpG **5** and Comparative Analysis of Synthetic Strategies.* The two tripeptide substrates for this study, AC-Me-cpG **3** and ACcpG **5**, were synthesized using distinct strategies, allowing evaluation and comparison of the two routes (Scheme 4).

AC-Me-cpG **3** was synthesized from the achiral starting material, 1-methylcyclopropanemethanol, according to previously described methodology (*18*, *23*). Oxidation by tetrapropylammonium perruthenate (TPAP) and *N*-methylmorpholine *N*-oxide (NMO) was followed by amination using 4,4′-dimethoxybenzhydrylamine, and treatment with trimethylsilyl cyanide to install the nascent carboxylate moiety (*23*). Acid hydrolysis gave racemic DL-β-methylcyclopropylglycine **6**, which was deprotected and coupled to a partially protected AC dipeptide, *N*-*tert*-butyloxycarbonyl-α-*p*-methoxybenzyl-δ-(L-α-aminoadipoyl)-*S*-benzhydryl-L-

Scheme 4: Synthetic Routes to AC-Me-cpG **3** and ACcpG **5**[a]

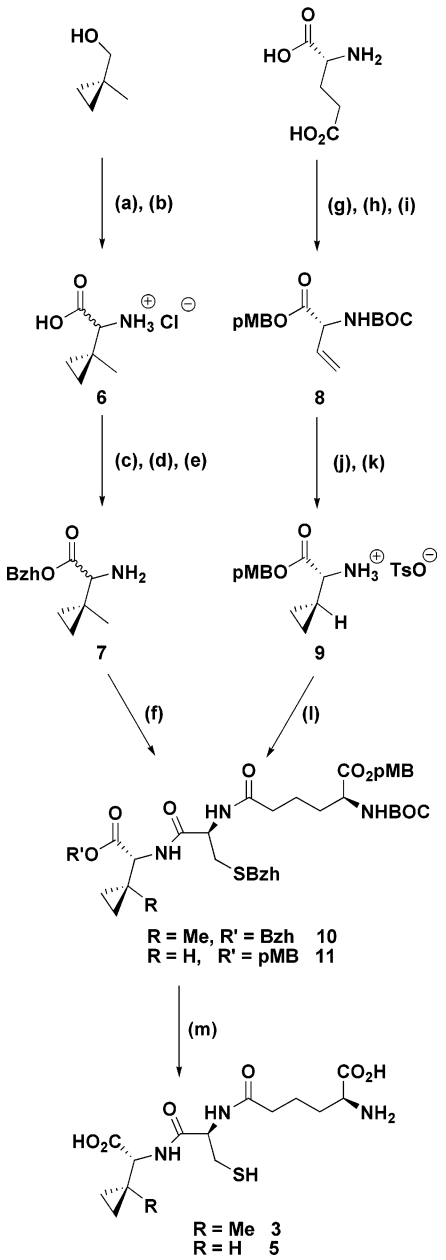

[a] (a) TPAP, NMO, 4 Å molecular sieves; (b) (i) 4,4′-dimethoxybenzhydrylamine, 4 Å molecular sieves, (ii) TMS-CN, (iii) HCl, quantitative over 2 steps; (c) $(BOC)_2O$, NaOH, 1,4-dioxane/water; (d) Ph_2CN_2, CH_3CN, 45% over 2 steps; (e) TsOH, EtOH/Et_2O; $NaHCO_3$ (aq), 93%; (f) *N-tert*-butyloxycarbonyl-α-*p*-methoxybenzyl-*δ*-(L-α-aminoadipoyl)-*S*-benzhydryl-L-cysteine, EEDQ, DCM, 21%; (g) $(BOC)_2O$, NaOH, *t*-BuOH/H_2O, quantitative; (h) *p*MB-Cl, Et_3N, DMF, 41%; (i) $Pb(OAc)_4$, $Cu(OAc)_2$ (cat.), benzene, 44%; (j) $Pd(OAc)_2$, CH_2N_2, Et_2O, 81%; (k) TsOH, EtOH/Et_2O, 95%; (l) *N-tert*-butyloxycarbonyl-α-*p*-methoxybenzyl-*δ*-(L-α-aminoadipoyl)-*S*-benzhydryl-L-cysteine, EDCI, HOBT, Et_3N, DCM, 37%; (m) (i) TFA, anisole; (ii) HPLC, 27% AC-Me-cpG **3**, 20% ACcpG **5**.

cysteine (*24*), using EEDQ methodology. This gave the fully protected tripeptide as a mixture of two diastereomers, from which the desired L,L,D-product **10** was isolated by chromatography as the less polar diastereomer (*23*) (stereochemistry further confirmed by crystallographic data). Global deprotection, using trifluoroacetic acid (TFA) and anisole, and HPLC purification afforded the desired product **3** (*18*).

Synthesis of ACcpG **5** utilized the method of Hanessian (*25*), which involves lead(IV)/copper(II)-mediated oxidative decarboxylation of a protected D-glutamic acid derivative. The resulting vinylglycine moiety **8** was subjected to palladium-catalyzed carbene insertion (*26*) to introduce the cyclopropyl species. Removal of the BOC group to give the cyclopropylglycine moiety **9** and coupling to the AC dipeptide using EDCI and HOBT (*27*) gave the protected tripeptide **11**. Global deprotection and purification by HPLC afforded the final ACcpG tripeptide **5**.

These two distinct methodologies were both successful in affording the cyclopropyl-bearing tripeptides. The demanding lead(IV)/copper(II)-mediated oxidative decarboxylation and carbene insertion reactions involved in the synthesis of **5** from D-glutamic acid resulted in a modest overall yield for this route. Since the method used for construction of AC-Me-cpG **3** utilized an achiral starting material and involved racemic synthetic intermediates, a large material loss was incurred upon separation of the tripeptide diastereomers. However, the good yield of the individual synthetic steps for incorporation of the amine and carboxylate functionalities resulted in a higher overall yield for this route, relative to that seen in construction of ACcpG **5**.

*Crystal Structures of AC-Me-cpG **3** and ACcpG **5** with IPNS.* The substrate analogues AC-Me-cpG **3** and ACcpG **5** were each cocrystallized with IPNS in the presence of Fe(II) under anaerobic conditions (*28*). Plate-shaped crystals were obtained of approximate dimensions 0.1 × 0.1 × 0.2 mm (ACcpG **5**) and 0.15 × 0.15 × 0.3 mm (AC-Me-cpG **3**). These crystals diffracted to 1.46 Å and 1.30 Å resolution, respectively, and were used to solve the X-ray crystal structures of the anaerobic IPNS−Fe(II)−(AC-Me-cpG) and IPNS−Fe(II)−ACcpG complexes (Figure 1A,B). Crystallographic statistics are presented in Table 1.

In both of these structures, the tripeptide substrate analogue lies in a similar extended conformation in the IPNS active site to that adopted by the natural substrate ACV **1** (Figure 1C). As seen in the IPNS−Fe(II)−ACV structure (*7*), the tripeptides are tethered to the protein through the cysteinyl sulfhydryl group, which is bound directly to the iron center. Similarly, a salt bridge is formed through the α-aminoadipoyl carboxylate to Arg_{187}, and a network of hydrogen bonds is formed through the "D-valinyl" carboxylate to Tyr_{189}, Ser_{281}, and (*via* a water molecule) Arg_{279}. The cysteinyl carbonyl groups point "forward", as in the anaerobic IPNS−Fe(II)−ACV structure (*7*), and the cyclopropyl moieties occupy the space normally taken by the D-valinyl isopropyl side chain of ACV **1**.

In comparison to the IPNS−Fe(II)−ACV complex, the IPNS−Fe(II)−ACcpG **5** structure has an additional water molecule bound to the iron in the oxygen-binding position, *trans* to Asp_{216} (Figure 1B). This phenomenon has been observed crystallographically before with substrate analogues that bear small side chains in this region, such as the methyl group of AC-D-alanine (*10*), the ethyl group of AC-D-α-aminobutyric acid (*11*), and the vinyl group of AC-D-vinylglycine (*8*). IPNS has been shown to mediate the oxidative turnover of some of these substrates in solution (*30*−*32*), reactions that presumably require an oxygen−water exchange equilibrium. The need for such an equilibrium has been offered as the explanation for an observed slower turnover of such substrate analogues by IPNS (*11*).

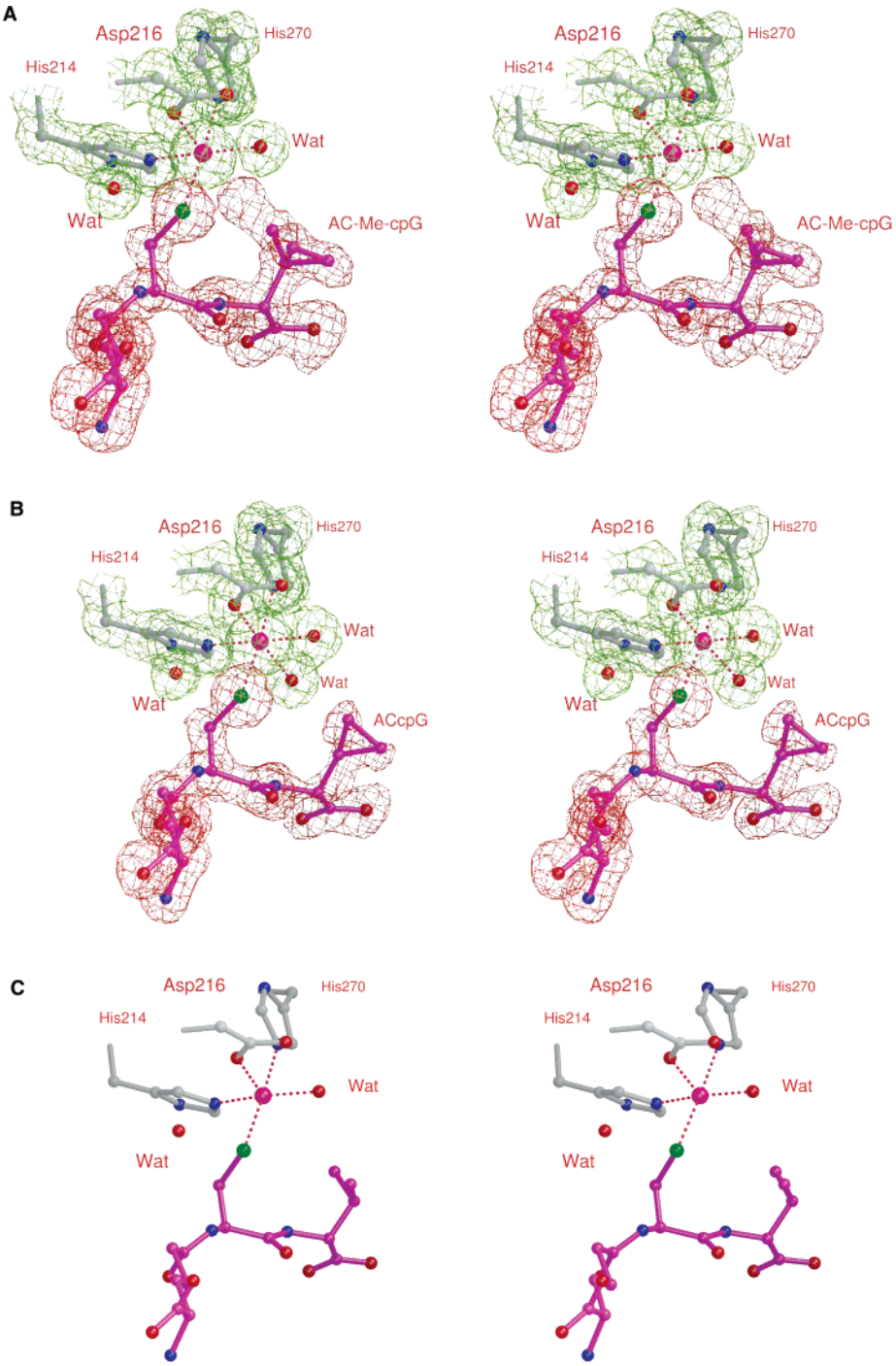

FIGURE 1: Stereo figures showing IPNS in complex with (A) AC-Me-cpG **3**; (B) ACcpG **5**; and (C) ACV **1**. In (A) and (B), $2mF_o-DF_c$ electron density maps (in green) are contoured at 1.0 σ around the protein atoms, and mF_o-DF_c omit difference maps (in red) are contoured at 3.0 σ around AC-Me-cpG **3** or ACcpG **5**.

The different geometric constraints of the cyclopropyl ring of ACcpG **5** (relative to ACV **1**) and the consequent subtle changes in geometry about the β-carbon must be sufficient to allow water in to bind to iron at this position in an analogous manner. Overall, however, the structure of ACcpG **5** in complex with IPNS (Figure 1B) shows the substrate bound in an orientation that should be compatible for oxidative turnover upon introduction of dioxygen.

The β-methyl group of AC-Me-cpG **3** points directly toward the iron center of IPNS (Figure 1A), which would allow for ready abstraction of a hydrogen radical from this methyl group by the putative IPNS iron(IV)−oxo intermediate during catalysis. Relative to the ACcpG **5** structure, this β-methyl group provides additional steric bulk around the oxygen-binding position *trans* to Asp_{216}, and thus would hinder the ability of water to bind. Like the D-valinyl isopropyl group of ACV **1**, the β-methylcyclopropyl group of AC-Me-cpG **3** likely assists in controlling the hydrophobicity of the oxygen-binding pocket.

However, unlike the ACV **1** structure (Figure 1C), it appears that the displacement of water from this position in the AC-Me-cpG **3** complex is incomplete. There is some additional electron density in the position *trans* to Asp_{216} in the IPNS−Fe(II)−AC-Me-cpG structure (Figure 1A). This

Table 1: Crystallographic Statistics for Anaerobic IPNS−Fe(II)−AC-Me-cpG and IPNS−Fe(II)−ACcpG Crystal Structures

	IPNS−Fe^{II}−AC-Me-cpG		IPNS−Fe^{II}−ACcpG	
X-ray source	ID14-EH2, ESRF		ID14-EH3, ESRF	
wavelength (Å)	0.933		0.935	
space group	$P2_12_12_1$		$P2_12_12_1$	
unit cell (*a*, *b*, *c*; Å)	46.7, 71.2, 100.9		46.6, 71.1, 100.7	
resolution shell (Å)	34.30−1.46	1.54−1.46	46.57−1.30	1.37−1.30
no. of reflns	232914	33490	353040	41310
no. of unique reflns	59159	8480	81160	11431
average $I/\sigma(I)$	9.7	3.3	13.4	3.1
completeness (%)	100.0	100.0	98.2	95.8
R_{merge} (%)[a]	13.6	35.1	7.6	39.2
R_{cryst} (%)[b]	14.2		13.2	
R_{free} (%)[c]	16.7		15.7	
RMS deviation[d]	0.010 (1.4)		0.008 (1.3)	
B factors (Å^2)[e]	11.0, 12.6, 14.6, 25.8		11.3, 14.4, 12.3, 24.8	
PDB ID	2IVJ		2IVI	

[a] $R_{merge} = \sum_j\sum_h|I_{h,j} - \langle I_h\rangle|/\sum_j\sum_h\langle I_h\rangle \times 100$. [b] $R_{cryst} = \sum||F_{obs}| - |F_{calc}||/\sum|F_{obs}| \times 100$. [c] R_{free} based on 4% of total reflections. [d] RMS deviation from ideality for bond lengths (Å) (bond angles (deg)). [e] Average *B* factors for main chain, side chain, substrate, and waters, respectively.

is likely due to partial occupancy of a water molecule ligated to the iron in this binding site, possibly due to less than full occupancy of the substrate. The presence of such a water ligand *trans* to Asp_{216} would presumably hinder the ability of oxygen to bind, as discussed above. An alternative explanation for this density would be an adventitious oxidation event of the β-methyl to a β-hydroxymethyl group. It is however hard to conceive of substrate oxidation (either enzyme-mediated or nonenzymatic) under the stringent anaerobic conditions of the experimental system. Moreover, it is difficult to rationalize such a hydroxylation process at an unactivated primary carbon center without prior oxidation of the cysteinyl portion of the substrate, particularly given the extensive precedent for reaction of IPNS through initial β-lactam formation prior to D-valinyl oxidation (*4*).

MECHANISTIC DISCUSSION

The *pro-S* bond of the cyclopropane of AC-Me-cpG **3** is known to be broken stereospecifically during IPNS-mediated turnover (*19*, *20*). Based on the crystal structure (Figure 2), it is likely that the orientation of the methylcyclopropyl group with respect to the proposed iron(IV)−oxo intermediate is responsible for this stereospecific control. Interactions with the residues surrounding the methylcyclopropyl group, including van der Waals interactions between the cyclopropane moiety and the hydrophobic residues lining that part of the active site, in particular Leu_{223} and Pro_{283}, hinder movement of this group, maintaining its orientation for stereospecific cyclopropane ring opening.

In the complex of IPNS with the native substrate ACV **1**, the D-valinyl group is known to rotate around its Cα−Cβ bond on binding of NO (and therefore presumably of dioxygen) to iron (*7*). This is necessary to allow space for the diatomic species to bind to the iron center, and also presents the D-valinyl β C−H bond toward the site of the iron(IV)−oxo intermediate. AC-Me-cpG **3** seems less likely to undergo an analogous rotation during reaction with IPNS, since there would be little or no relief of steric compression with this substrate analogue. In particular, rotation appears unlikely to create additional space for binding of oxygen to the iron.

At this juncture, it is apparent that the previously proposed mechanisms for IPNS-mediated turnover of cyclopropyl-bearing substrate **3** (Scheme 3) are inadequate to explain our current data. In the IPNS−Fe(II)−(AC-Me-cpG) structure (Figure 2), the *pro-R* bond of the cyclopropyl group overlays the position of the D-valinyl β C−H bond of ACV, while the *pro-S* bond is oriented away from the iron (Figure 2). In this orientation, reaction of the iron(IV)−oxo species with the *pro-S* bond by the "ene"-type mechanism proposed (Scheme 3) is not possible, and reaction *via* the C−H bond insertion mechanism (Scheme 3) would presumably also require rearrangement. Thus, in light of the X-ray crystal structure, the two possible mechanistic pathways postulated in the absence of any crystallographic information (*18*) seem unlikely.

In line with current understanding of the mechanism of IPNS with its natural substrate ACV **1** (Scheme 2A), we suggest an alternative mechanism for the reaction of IPNS with AC-Me-cpG **3** (Scheme 2B). The initial stages of turnover most likely give formation of the β-lactam ring, following the established route for the reaction of ACV **1** and other substrate analogues (*4*). We then propose a radical pathway, in which a hydrogen atom is abstracted from the β-methyl group of **3** by the nascent iron(IV)−oxo intermedi-

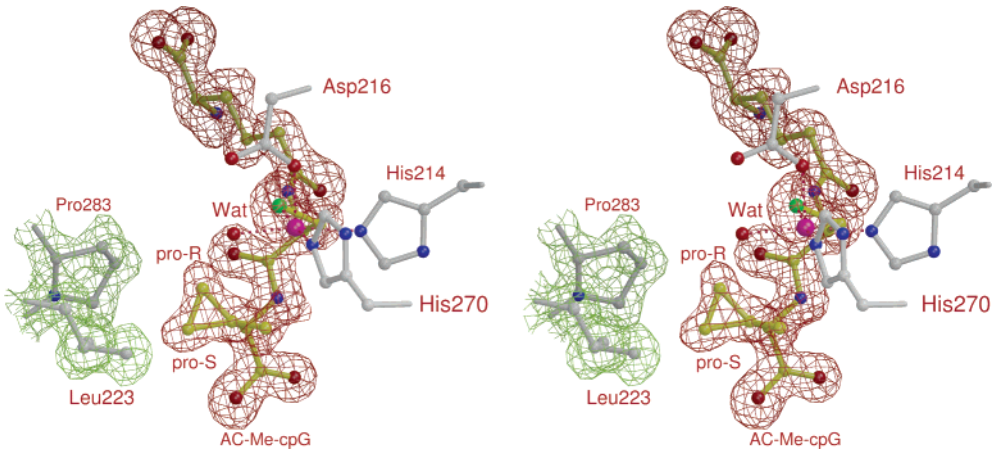

FIGURE 2: Stereo figure showing the positioning of the *pro-R* and *pro-S* bonds of the cyclopropyl group of AC-Me-cpG **3** relative to the iron center of IPNS. A $2mF_o-DF_c$ electron density map (in green) is contoured at 1.0 σ around the protein atoms, and an mF_o-DF_c omit difference map (in red) is contoured at 3.0 σ around AC-Me-cpG **3**.

ate. This would be analogous to the first step of a radical-based hydroxylation reaction, common in the related 2-oxoglutarate-dependent dioxygenases. However, the hydrogen abstraction here is likely accompanied by rapid cyclopropyl ring opening. It can be seen from the structure that, if this process is concerted, then the *pro-S* bond that is broken is *anti* to the abstracted hydrogen. Following ring opening, only a rotation around the formerly *pro-R* bond (Figure 2) is required to allow closure of the homoallylic radical onto sulfur to give the (*4*, *7*)-bicyclic system **4** (Scheme 2B). (It is also possible that, by rotation around the Cα−Cβ bond, the hydroxylation process is completed to give a primary hydroxyl group, which is then displaced by nucleophilic substitution of the sulfur, with water acting as a leaving group. However, the single step radical closure onto sulfur is more appealing as it requires less movement within the active site.)

While non-heme iron oxidases are known to perform a wide variety of reactions, no evidence for a bond between the iron and a substrate carbon atom has yet been obtained. In contrast, many reactions involving hydrogen abstraction or hydroxylation have been documented (*29*). Our alternative mechanism avoids the need to invoke an iron−carbon bond (as had been previously proposed as an intermediate during AC-Me-cpG **3** turnover by IPNS, Scheme 3) and is in accord with current mechanistic understanding of IPNS (Scheme 2A) (*7*) and other non-heme iron enzymes.

It is intriguing to note that, despite the structural similarity of these two substrate analogues, ACcpG **5** does not appear to be turned over by IPNS (Domayne-Hayman, B. P., and Baldwin, J. E., unpublished) while AC-Me-cpG **3** reacts readily (*18*). Although ACcpG **5** lacks the primary methyl group of tripeptide **3** (from which the hydrogen is putatively abstracted by the enzyme-bound iron(IV)−oxo intermediate), the β-lactam-forming region of compound **5** is identical to AC-Me-cpG **3** and the native substrate ACV **1**. ACcpG **5** also possesses several secondary and tertiary carbon centers that may be possible sites for hydrogen abstraction by an equivalent iron(IV)−oxo intermediate. Such cyclopropyl carbon−hydrogen bonds are however considerably stronger than the equivalent bonds of the D-valinyl isopropyl side chain of ACV **1**.

ACcpG **5** is of similar size to ACV **1**; however, the altered geometry of the three-membered ring appears sufficient to permit water to enter and bind at the iron coordination site *trans* to Asp_{216}, which does not occur with ACV **1**. We postulate that the bulk and rigidity of the cyclopropyl group lead to active site crowding in the presence of the additional iron-bound water ligand. This steric crowding might kinetically hinder the exchange of the water molecule for dioxygen, a plausible explanation for the observed inability of IPNS to catalyze oxidative turnover of ACcpG **5**. By contrast, in the IPNS−Fe(II)−(AC-Me-cpG) structure, only partial occupancy by a water molecule is seen at this site (Figure 1A). Such partial occupancy suggests lower affinity of this water ligand for iron relative to that of the IPNS−Fe(II)−ACcpG complex. That turnover of AC-Me-cpG **3** by IPNS is observed (*18*), while ACcpG **5** is not turned over (Domayne-Hayman, B. P., and Baldwin, J. E., unpublished), is likely due to more ready exchange of this iron-bound water with oxygen in the IPNS complex of **3**.

The crystal structures of IPNS in complex with AC-Me-cpG **3** and ACcpG **5** presented here allow revision of the mechanism for the turnover of AC-Me-cpG **3** by IPNS. This radical-based mechanism takes into account the observed orientation of substrates **3** and **5** in the IPNS active site, primed for reaction upon introduction of dioxygen, and incorporates current understanding of the native mechanism of IPNS and related 2-oxoglutarate-dependent non-heme iron oxidase enzymes.

ACKNOWLEDGMENT

We would like to thank the scientists at the ESRF, Grenoble, for technical assistance.

REFERENCES

1. Baldwin, J. E., and Schofield, C. J. (1992) in *The Chemistry of β-Lactams* (Page, M. I., Ed.) pp 1−78, Blackie Academic & Professional, London.
2. White, R. L., John, E.-M. M., Baldwin, J. E., and Abraham, E. P. (1982) Stoichiometry of Oxygen Consumption in the Biosynthesis of Isopenicillin From a Tripeptide, *Biochem. J. 203*, 791−793.
3. Baldwin, J. E., Adlington, R. M., Moroney, S. E., Field, L. D., and Ting, H.-H. (1984) Stepwise Ring Closure in Penicillin Biosynthesis. Initial β-Lactam Formation, *J. Chem. Soc., Chem. Commun.* 984−986.
4. Burzlaff, N. I., Rutledge, P. J., Clifton, I. J., Hensgens, C. M. H., Pickford, M., Adlington, R. M., Roach, P. L., and Baldwin, J. E. (1999) The Reaction Cycle of Isopenicillin *N* Synthase Observed by X-Ray Diffraction, *Nature 401*, 721−724.
5. Roach, P. L., Schofield, C. J., Baldwin, J. E., Clifton, I. J., and Hajdu, J. (1995) Crystallization and Preliminary X-Ray Diffraction Studies on Recombinant Isopenicillin N Synthase From *Aspergillus nidulans*, *Protein Sci. 4*, 1007−1009.
6. Roach, P. L., Clifton, I. J., Fülöp, V., Harlos, K., Barton, G. J., Hajdu, J., Andersson, I., Schofield, C. J., and Baldwin, J. E. (1995) Crystal Structure of Isopenicillin N Synthase is the First From a New Structural Family of Enzymes, *Nature 375*, 700−704.
7. Roach, P. L., Clifton, I. J., Hensgens, C. M. H., Shibata, N., Schofield, C. J., Hajdu, J., and Baldwin, J. E. (1997) Structure of Isopenicillin *N* Synthase Complexed with Substrate and the Mechanism of Penicillin Formation, *Nature 387*, 827−830.
8. Elkins, J. M., Rutledge, P. J., Burzlaff, N. I., Clifton, I. J., Adlington, R. M., Roach, P. L., and Baldwin, J. E. (2003) Crystallographic Studies on the Reaction of Isopenicillin N Synthase with an Unsaturated Substrate Analogue, *Org. Biomol. Chem. 1*, 1455−1460.
9. Grummitt, A. R., Rutledge, P. J., Clifton, I. J., and Baldwin, J. E. (2004) Active Site Mediated Elimination of Hydrogen Fluoride From a Fluorinated Substrate Analogue by Isopenicillin N Synthase, *Biochem. J. 382*, 659−666.
10. Long, A. J., Clifton, I. J., Roach, P. L., Baldwin, J. E., Rutledge, P. J., and Schofield, C. J. (2005) Structural Studies on the Reaction of Isopenicillin N Synthase with the Truncated Substrate Analogues δ-(L-α-Aminoadipoyl)-L-Cysteinyl-Glycine and δ-(L-α-Aminoadipoyl)-L-Cysteinyl-D-Alanine, *Biochemistry 44*, 6619−6628.
11. Long, A. J., Clifton, I. J., Roach, P. L., Baldwin, J. E., Schofield, C. J., and Rutledge, P. J. (2003) Structural Studies on the Reaction of Isopenicillin N Synthase with the Substrate Analogue δ-(L-α-Aminoadipoyl)-L-Cysteinyl-D-α-Aminobutyrate., *Biochem. J. 372*, 687−693.
12. Ogle, J. M., Clifton, I. J., Rutledge, P. J., Elkins, J. M., Burzlaff, N. I., Adlington, R. M., Roach, P. L., and Baldwin, J. E. (2001) Alternative Oxidation by Isopenicillin *N* Synthase Observed by X-Ray Diffraction, *Chem. Biol. 8*, 1231−1237.
13. Howard-Jones, A. R., Rutledge, P. J., Clifton, I. J., Adlington, R. M., and Baldwin, J. E. (2005) Unique Binding of a Non-Natural L,L,L-Substrate by Isopenicillin N Synthase, *Biochem. Biophys. Res. Commun. 336*, 702−708.
14. Daruzzaman, A., Clifton, I. J., Adlington, R. M., Baldwin, J. E., and Rutledge, P. J. (2006) Unexpected Oxidation of a Depsipeptide Substrate Analogue in Crystalline Isopenicillin N Synthase, *ChemBioChem 7*, 351−358.

15. Que, L. J., and Ho, R. Y. N. (1996) Dioxygen Activation by Enzymes with Mononuclear Non-Heme Iron Active Sites, *Chem. Rev. 96*, 2607−2624.
16. Cooper, R. D. G. (1993) The Enzymes Involved in Biosynthesis of Penicillin and Cephalosporin; Their Structure and Function, *Bioorg. Med. Chem. 1*, 1−17.
17. Baldwin, J. E., and Bradley, M. (1990) Isopenicillin N Synthase: Mechanistic Studies, *Chem. Rev. 90*, 1079−1088.
18. Baldwin, J. E., Adlington, R. M., Domayne-Hayman, B. P., Knight, G., and Ting, H.-H. (1987) Use of the Cyclopropylcarbinyl Test to Detect a Radical-Like Intermediate in Penicillin Biosynthesis, *J. Chem. Soc., Chem. Commun.* 1661−1663.
19. Baldwin, J. E., Adlington, R. M., Marquess, D. G., Pitt, A. R., and Russell, A. T. (1991) Evidence for an Insertion-Homolysis Mechanism for Carbon-Sulphur Bond Formation in Penicillin Biosynthesis, *J. Chem. Soc, Chem. Commun. 13*, 856−858.
20. Baldwin, J. E., Adlington, R. M., Marquess, D. G., Pitt, A. R., Porter, M. J. and Russell, A. T. (1996) Evidence for an Insertion-Homolysis Mechanism for Carbon-Sulphur Bond Formation in Penicillin Biosynthesis; 2. Incubation and Interpretation, *Tetrahedron 52*, 2537−2556.
21. Brownlee, K. A., Delves, C. S., Dorman, M., Green, C. A., Grenfell, E., Johnson, J. D. A., and Smith, N. (1947) The Biological Assay of Streptomycin By a Modified Cylinder Plate Method, *J. Gen. Microbiol. 53*, 40−53.
22. Solomon, E. I. (2001) Geometric and Electronic Structure Contributions to Function in Bioinorganic Chemistry: Active Sites in Non-Heme Iron Enzymes, *Inorg. Chem. 40*, 3656−3669.
23. Baldwin, J. E., Adlington, R. M., Marquess, D. G., Pitt, A. R., Porter, M. J., and Russell, A. T. (1996) Evidence for an Insertion-Homolysis Mechanism for Carbon-Sulphur Bond Formation in Penicillin Biosynthesis; 1. Synthesis of Tripeptide Probes, *Tetrahedron 52*, 2515−2536.
24. Baldwin, J. E., Herchen, S. R., Johnson, B. L., Jung, M., Usher, J. J., and Wan, T. (1981) Synthesis of δ-(L-α-Aminoadipoyl)-L-Cysteinyl-D-Valine and Some Carbon-13 and Nitrogen-15 Labelled Isotopomers, *J. Chem. Soc., Perkin Trans. 1* 2253−2257.
25. Hanessian, S., and Sahoo, S. P. (1984) A Novel and Efficient Synthesis of L-Vinylglycine, *Tetrahedron Lett. 35*, 1425−1428.
26. Paulissen, R., Hubert, A. J., and Teyssie, P. (1972) Transition Metal Catalysed Cyclopropanation of Olefin, *Tetrahedron Lett. 13*, 1465−1466.
27. König, W., and Geiger, R. (1970) A New Method For Synthesis of Peptides: Activation of the Carboxyl Group with Dicyclohexylcarbodiimide Using 1-Hydroxybenzotriazoles as Additives, *Chem. Ber. 103*, 788−798.
28. Roach, P. L., Clifton, I. J., Hensgens, C. M. H., Shibata, N., Long, A. J., Strange, R. W., Hasnain, S. S., Schofield, C. J., Baldwin, J. E., and Hajdu, J. (1996) Anaerobic Crystallization of an Isopenicillin N Synthase Fe(II) Substrate Complex Demonstrated By X-Ray Studies, *Eur. J. Biochem. 242*, 736−740.
29. Costas, M., Mehn, M. P., Jensen, M. P., and Que, L. J. (2004) Dioxygen Activation at Mononuclear Nonheme Iron Active Sites: Enzymes, Models, and Intermediates, *Chem. Rev. 104*, 939−986.
30. Baldwin, J. E., Abraham, E. P., Adlington, R. M., Chakravarti, B., Derome, A. E., Murphy, J. A., Field, L. D., Green, N. B., Ting, H.-H., and Usher, J. J. (1983) Penicillin Biosynthesis. Dual Pathways From a Modified Substrate, *J. Chem. Soc., Chem. Commun.* 1317−1319.
31. Bahadur, G. A., Baldwin, J. E., Usher, J. J., Abraham, E. P., Jayatilake, G. S., and White, R. L. (1981) Cell-Free Biosynthesis of Penicillins. Conversion of Peptides Into New β-Lactam Antibiotics, *J. Am. Chem. Soc. 103*, 7650−7651.
32. Baldwin, J. E., Adlington, R. M., Basak, A., Flitsch, S. L., Forrest, A. K., and Ting, H.-H. (1986) Penicillin Biosynthesis: Structure-Reactivity Profile of Unsaturated Substrates For Isopenicillin N Synthetase, *J. Chem. Soc., Chem. Commun.* 273−275.
33. Bodansky, M., and Bodansky, A. (1984) *The Practice of Peptide Synthesis*, 2nd ed., Springer-Verlag, Berlin.
34. Kochi, J. K., Bacha, J. D., and Bethea, T. W. I. (1967) Free Radicals in Thermal and Photochemical Oxidative Decarboxylations With Lead(IV), *J. Am. Chem. Soc. 89*, 6538−6547.
35. Kochi, J. K., and Bacha, J. D. (1968) Solvent Effects On the Oxidation of Alkyl Radicals By Lead(IV) and Copper(II) Complexes, *J. Org. Chem. 33*, 2746−2754.
36. Kochi, J. K. (1965) Oxidations with Lead(IV). I Mechanism of the Decarboxylation of Pentanoic Acids, *J. Am. Chem. Soc. 87*, 3609−3619.
37. Kapps, M., and Kirmse, W. (1969) Katalysierte Reaktionen des Diazomethans mit Vinyloxiran, *Angew. Chem. 81*, 86.
38. Kirmse, W., and Kapps, M. (1968) Reaktionen des Diazomethans mit Diallylsulfid und Allyläthern unter Kupfersalz-Katalyse, *Chem. Ber. 101*, 994−1003.
39. Mojsov, S., Mitchell, A. R., and Merrifield, R. B. (1980) A Quantitative Evaluation of Methods For Coupling Asparagine, *J. Org. Chem. 45*, 555−560.
40. Leslie, A. G. W. (1999) Integration of Macromolecular Diffraction Data, *Acta Crystallogr. D 55*, 1696−1702.
41. Collaborative Computational Project, Number 4 (1994) The *CCP4* Suite: Programs For Protein Crystallography, *Acta Crystallogr. D 50*, 760−763.
42. Jones, T. A., Zou, J. Y., Cowan, S. W., and Kjelgaard, M. (1991) Improved Methods For Building Protein Models in Electron Density Maps and the Location of Errors in These Models, *Acta Crystallogr. A 47*, 110−119.

BI062314Q